The Structure of Hexamethyltungsten, $W(CH_3)_6$: Distorted Trigonal Prismatic with C_3 Symmetry

Martin Kaupp

Contribution from the Institut für Theoretische Chemie, Universität Stuttgart, Pfaffenwaldring 55, D-70569 Stuttgart, Germany, and Max-Planck-Institut für Festkörperforschung, Heisenbergstrasse 1, D-70569 Stuttgart, Germany

Received July 7, 1995. Revised Manuscript Received January 2, 1996[⊗]

Abstract: Ab initio and density functional calculations show that the equilibrium structure of hexamethyltungsten is a distorted trigonal prism of C_3 symmetry (with local C_{3v} symmetry for the WC_6 skeleton). A regular prismatic D_3 structure (with D_{3h} skeleton) is found to be ca. 20 kJ mol^{-1} higher in energy at correlated levels of theory. It is a transition state connecting two C_3 minima. These results extend a recent gas-phase electron diffraction study which favored a regular prismatic structure but could not rule out a distortion to C_{3v}. The failure of a previous theoretical study to locate the distorted minimum is due to the neglect of electron correlation and to some other restrictions during the structure optimizations. Correlation is important, e.g. for the description of hyperconjugative "agostic" C−H → W interactions which are found to be pronounced in $W(CH_3)_6$. Structures optimized with gradient-corrected or hybrid density functionals, or at the MP2 level, describe these interactions well. The observed single-line ^{13}C and ^{1}H NMR spectra are explained by dynamic motions due to the low D_3 inversion and methyl rotation barriers. ^{13}C chemical shifts calculated using density functional theory differ by ca. 18 ppm between the two nonequivalent sets of methyl groups in the distorted trigonal prismatic structure. Low-temperature NMR experiments could be useful to confirm this value and thus the distortion. Harmonic vibrational frequency analyses are consistent with experimental results and have been used to characterize stationary points on the potential energy surface. Differences between the structural preferences of $W(CH_3)_6$ and WH_6 are investigated via detailed bonding analyses.

I. Introduction

It has become clear during the past 5−10 years that many d^0 metal complexes favor less symmetrical structures than those predicted by simple valence-shell electron-pair-repulsion (VSEPR) or electrostatic models of structural chemistry.[1−12] Thus, dicoordinate d^0 MX_2 complexes often are bent instead of linear,[1−4] tricoordinate species may be pyramidal rather than planar,[3−6] the dihydride dimers M_2H_4 (M = Sr, Ba) and related species favor completely unexpected C_{3v} structures,[5,7] and MX_5 species may adopt square-pyramidal instead of trigonal-bipyramidal coordination.[8] σ-Bonding interactions involving metal d-orbitals and the polarization of the metal penultimate $(n - 1)$ p-shell have been shown to favor the less symmetrical coordination environments in this type of d^0 complex. In contrast, electrostatic repulsion between the ligands and π-bonding contributions (in the presence of occupied orbitals on the ligands with suitable symmetry) both favor more symmetrical coordination.[1−5,8−10]

What is perhaps most fascinating is that even octahedral symmetry, which is so predominant in transition metal chemistry, may be unfavorable for purely σ-bound d^0 MX_6 species. This has been shown by ab initio calculations on hexahydride species like MH_6^{2-} (M = Ti, Zr) or MH_6 (M = Cr, W),[8−12] by X-ray diffraction for the $Zr(CH_3)_6^{2-}$ anion,[11] and recently both by experiment (gas-phase electron diffraction, GED)[12] and by ab initio calculations[8] for hexamethyltungsten, $W(CH_3)_6$. Calculations for WH_6 suggest a distorted trigonal prism (C_{3v}) as global minimum (with a C_{5v} structure close in energy).[8,9] In contrast, for $W(CH_3)_6$ Kang et al. proposed a regular trigonal prismatic D_{3h} arrangement, based on pseudopotential Hartree−Fock structure optimizations with subsequent MP2 single-point calculations.[8] They failed to locate a distorted prismatic C_{3v} structure analogous to the one found for WH_6[8,9] and argued that the greater steric bulk of the methyl compared to the hydride ligands prevents the symmetry lowering. The GED results were

[⊗] Abstract published in *Advance ACS Abstracts,* March 1, 1996.

(1) (a) Kaupp, M.; Schleyer, P. v. R.; Stoll, H.; Preuss, H. *J. Chem. Phys.* **1991**, *94*, 1360. (b) Kaupp, M.; Schleyer, P. v. R.; Stoll, H.; Preuss, H. *J. Am. Chem. Soc.* **1991**, *113*, 6012. (c) Seijo, J.; Barandiaran, Z.; Huzinaga, S. *J. Chem. Phys.* **1991**, *94*, 762. (d) Kaupp, M.; Schleyer, P. v. R. *J. Am. Chem. Soc.* **1992**, *114*, 491. (e) Mösges, G.; Hampel, F.; Kaupp, M.; Schleyer, P. v. R. *J. Am. Chem. Soc.* **1992**, *114*, 10880. (f) For the first experimentally observed bent structure of an unsolvated, monomeric dialkyl−ytterbium(II) compound, cf.: Eaborn, C.; Hitchcock, P. B.; Izod, K.; Smith, J. D. *J. Am. Chem. Soc.* **1994**, *116*, 12071. (g) Many further references may be found in refs. 1a,b and 2a.

(2) (a) Kaupp, M.; Schleyer, P. v. R.; Stoll, H.; Dolg, M. *J. Am. Chem. Soc.* **1992**, *114*, 8202. (b) Kaupp, M.; Charkin, O. P.; Schleyer, P. v. R. *Organometallics* **1992**, *11*, 2767.

(3) (a) Kaupp, M.; Schleyer, P. v. R. *J. Phys. Chem.* **1992**, *96*, 7316. (b) Bauschlicher, C. W., Jr.; Sodupe, M.; Partridge, H. *J. Chem. Phys.* **1992**, *96*, 4453.

(4) (a) Jolly, C. A.; Marynick, D. S. *Inorg. Chem.* **1989**, *28*, 2893. (b) Siegbahn, P. E. M. *J. Phys. Chem.* **1993**, *97*, 9096. (c) Musaev, D. G.; Charkin, O. P. *Koordinat. Khim.* **1989**, *15*, 161. Also see: (d) Ghotra, J. S.; Hursthouse, M. B.; Welch, A. J. *J. Chem. Soc., Chem. Commun.* **1973**, 669. (e) Andersen, R. A.; Templeton, D. H.; Zalkin, A. *Inorg. Chem.* **1978**, *17*, 2317.

(5) Kaupp, M.; Schleyer, P. v. R. *J. Am. Chem. Soc.* **1993**, *115*, 11202.

(6) Westerhausen, M.; Schwarz, W. *Z. Anorg. Allg. Chem.* **1991**, *604*, 127. Westerhausen, M.; Schwarz, W. *Z. Anorg. Allg. Chem.* **1991**, *606*, 177. Vaarstra, B. A.; Huffman, J. C.; Streib, W. E.; Caulton, K. G. *Inorg. Chem.* **1991**, *30*, 121.

(7) (a) Drake, S. R.; Streib, W. E.; Folting, K.; Chisholm, M. H.; Caulton, K. G. *Inorg. Chem.* **1992**, *31*, 3205. (b) Westerhausen, M. *J. Organomet. Chem.* **1994**, *479*, 141.

(8) Kang, S. K.; Tang, H.; Albright, T. A. *J. Am. Chem. Soc.* **1993**, *115*, 1971.

(9) Shen, M.; Schaefer, H. F., III; Partridge, H. *J. Chem. Phys.* **1993**, *98*, 508.

(10) (a) Kang, S. K.; Albright, T. A.; Eisenstein, P. *Inorg. Chem.* **1989**, *28*, 1611. (b) Jonas, V.; Frenking, G.; Gauss, J. *Chem. Phys. Lett.* **1992**, *194*, 109.

(11) Morse, P. M.; Girolami, G. S. *J. Am. Chem. Soc.* **1989**, *111*, 4114.

(12) Haaland, A.; Hammel, A.; Rypdal, K.; Volden, H. V. *J. Am. Chem. Soc.* **1990**, *112*, 4547.

0002-7863/96/1518-3018$12.00/0

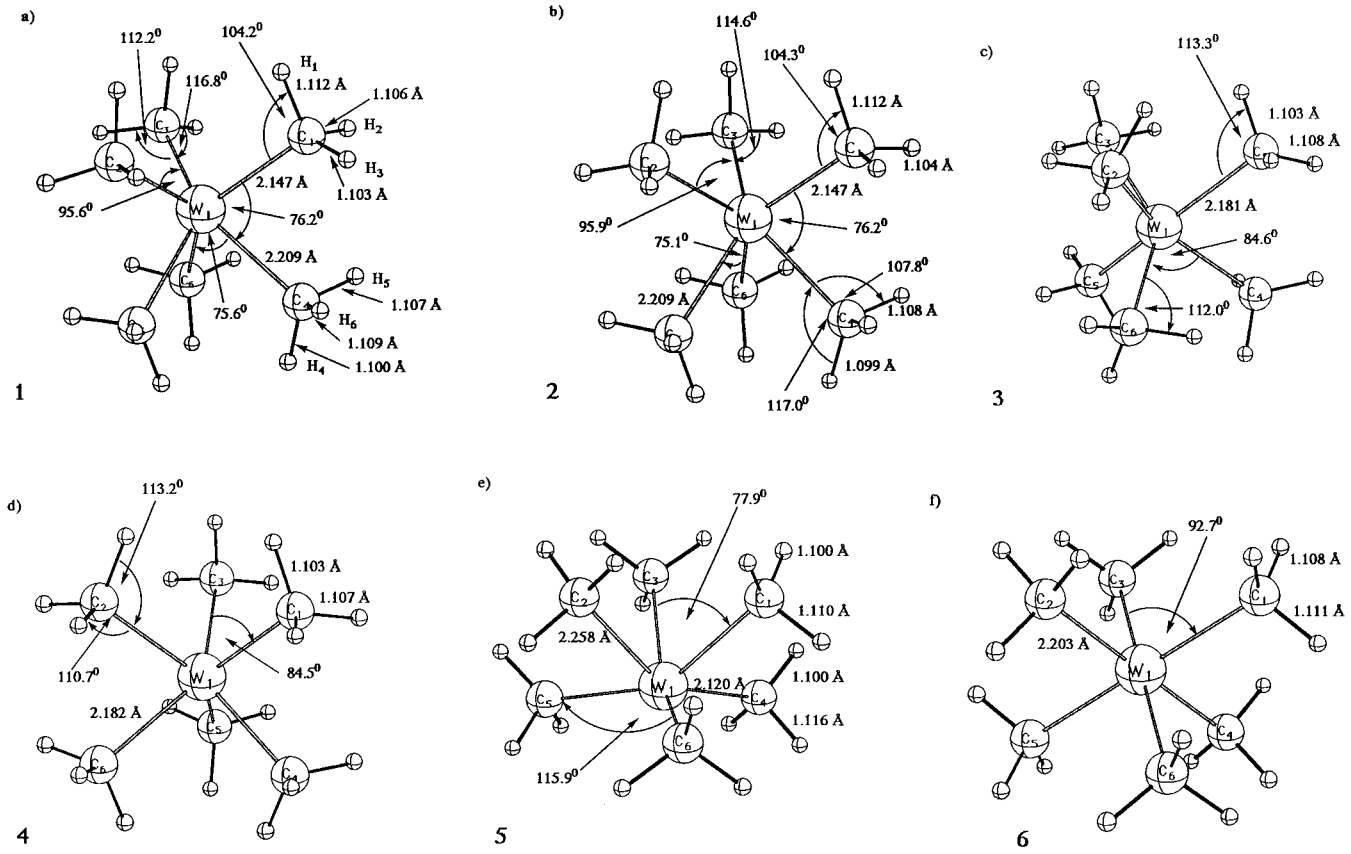

Figure 1. Atom numbering and BP86/A optimization results for different stationary points on the $W(CH_3)_6$ potential energy surface: (a) C_3 **1**, metal−hydrogen distances (in Å) are 2.649, 2.762, 2.821, 2.883, 2.780, 2.726 for H1 through H6; (b) C_{3v}, "distorted trigonal prismatic **2**; (c) D_3 **3**; (d) D_{3h} **4**; (e) C_{3v} "distorted octahedral" **5**; (f) D_{3d}, "octahedral" **6**.

also interpreted using a D_{3h} model, but distortion to C_{3v} could not be ruled out.[12] A molecular-mechanics approach incorporating valence-bond elements by Landis et al.[13] suggests a distorted structure, but less distorted than for WH_6.

As an experimentally accessible molecule,[12,14] hexamethyltungsten occupies a particularly important role in establishing the general validity of the above mentioned unusual coordination preferences for hexacoordinate d^0 species. We have therefore decided to conclusively settle the question of the true minimum structure of $W(CH_3)_6$ by computational reevaluation. The structure optimizations of Kang et al.[8] neglect electron correlation and restrict all C−H distances to be equal. However, hyperconjugative "agostic" interactions between C−H bonds and Lewis-acidic centers like W^{VI} may be important, and electron correlation (and C−H bond relaxation) may have to be included for a proper description. Therefore, we have used both MP2 calculations and two different density functional theory (DFT) methods for the structure optimizations, and additionally CCSD(T) energy calculations. Harmonic vibrational frequency analyses at correlated (DFT) levels have been carried out to clearly characterize the nature of the stationary points on the $W(CH_3)_6$ potential energy surface. Indeed, when electron correlation is included, a distorted C_3 structure is found to be lower in energy than a regular prismatic D_3 arrangement which is only a transition state. Computed NMR chemical shifts are given which might facilitate the experimental confirmation of our findings by low-temperature NMR spectroscopy. The importance of agostic interactions and the IR spectrum of $W(CH_3)_6$ are also discussed, and the electronic structures of WH_6 and $W(CH_3)_6$ are compared.

II. Computational Methods

Different stationary points **1**−**6** on the $W(CH_3)_6$ potential-energy surface (see Figure 1) have been considered at various theoretical levels. Initial DFT structure optimizations, with Becke's and Perdew's gradient-corrected exchange and correlation functionals (denoted BP86 in the following),[15] employed no symmetry and used auxiliary basis sets to fit electron density and exchange-correlation functional. These calculations were carried out with a modified version of the deMon program.[16] All optimizations used quasirelativistic effective-core potentials for both tungsten[17] and carbon.[18] The GTO valence basis sets were of the sizes (8s7p6d)/[6s5p3d][17] and (4s4p1d)/[2s2p1d][18] for W and C, respectively. A double-ζ basis was used for hydrogen.[19] In the following, this basis-set combination will be designated "A". The transferability of ab initio ECPs into DFT applications has been found to be excellent for ECP core sizes like those used in the present study.[20,21] The deMon optimizations converged to structures close to **1** (Figure 1a) when started from any initial guess with roughly trigonal-prismatic symmetry, and to structure **5** (Figure 1e) when starting from octahedral arrangements.

(13) Landis, C. R.; Cleveland, T.; Firman, T. K. *J. Am. Chem. Soc.* **1995**, *117*, 1859.

(14) (a) Galver, A. L.; Wilkinson, G. *J. Chem. Soc., Dalton Trans.* **1976**, 2235. (b) Shortland, A. J.; Wilkinson, G. *J. Chem. Soc., Dalton Trans.* **1973**, 872.

(15) (a) Becke, A. D. *Phys. Rev.* **1988**, *A38*, 3098. (b) Perdew, J. P. *Phys. Rev.* **1986**, *B33*, 8822.

(16) Salahub, D. R.; Fournier, R.; Mlynarski, P.; Papai, I.; St-Amant, A.; Ushio, J. In *Density Functional Methods in Chemistry*; Labanowski, J. K., Andzelm, J. W., Eds.; Springer: New York, 1991; p 77. St-Amant, A.; Salahub, D. R. *Chem. Phys. Lett.* **1990**, *169*, 387. St-Amant, A. Thesis, Université de Montréal, 1992.

(17) Andrae, D.; Häussermann, U.; Dolg, M.; Stoll, H.; Preuss, H. *Theor. Chim. Acta* **1990**, *77*, 123.

(18) Bergner, A.; Dolg, M.; Küchle, W.; Stoll, H.; Preuss, H. *Mol. Phys.* **1993**, *80*, 1431.

(19) Godbout, N.; Salahub, D. R.; Andzelm, J.; Wimmer, E. *Can. J. Chem.* **1992**, *70*, 560.

(20) Kaupp, M.; Flad, H.-J.; Köster, A.; Stoll, H.; Salahub, D. R. Unpublished results.

(21) van Wüllen, C. *Int. J. Quantum Chem.* In press.

Table 1. Relative Energies (kJ mol^{-1}) and Number of Imaginary Vibrational Frequencies for Different Stationary Points of $W(CH_3)_6$[a]

method[b]	C_3 (**1**)	C_{3v} ecl (**2**)	D_3 (**3**)	D_{3h} (**4**)	C_{3v} stg (**5**)	D_{3d} (**6**)
BP86/A//BP86/A	0.0	3.2	+24.6	+25.2	+131.9	+374.7
MP2/A//MP2/A	0.0	+0.6	+13.2	+13.3		
B3P86/A//B3P86/A		(0.0)		(+18.3)		
HF/B//BP86/A		(+14.2)		(0.0)	(+186.0)	(+625.8)
MP2/B//BP86/A		(0.0)		(+22.2)	(+118.0)	(+418.6)
CCSD/B//BP86/A		(0.0)		(+12.1)	(+134.1)	(+344.9)
CCSD(T)/B//BP86/A		(0.0)		(+17.5)	(+124.3)	(+366.1)
n-imag(BP86/A)[c]	0	3	1	4	1	10
ZPE(BP86/A)[d]	555.2	553.2	554.3	548.0	554.2	518.1

[a] See Figure 1 for the structures. Values in parentheses indicate that (presumably global-minimum) structure **1** (or **3** for HF) has not been calculated at this level. [b] See computational details section. [c] Number of imaginary frequencies. [d] Zero-point vibrational energy.

Based on these deMon results, optimizations utilizing symmetry but no fitting techniques were performed with the same pseudopotentials and valence basis sets, using the Gaussian92/DFT program.[22] These optimizations either employed the above mentioned BP86 functional[15] (the agreement with the deMon results for a given structure **1** or **5** was essentially perfect), a DFT/HF hybrid functional composed of Becke's 3-parameter exchange functional[23] plus Perdew's 1986 correlation functional[15b] (B3P86), or electron correlation was included at the second-order perturbation theory (MP2) level.

Different integration grids were tested in the DFT calculations. The default grid provided in Gaussian92/DFT[22] was of sufficient accuracy for the ECP optimizations, in good agreement with "FINE" grid[16] deMon results. However, to avoid spurious (small, ca. 100 cm^{-1}) imaginary frequencies in the vibrational analyses, the int=finegrid option of the Gaussian92/DFT program[22] had to be used (the structures were virtually unaffected by changes in the grid). All electrons outside the ECP cores were included in the active space for the MP2 (and coupled cluster, cf. below) calculations. Harmonic vibrational frequency analyses with Gaussian92/DFT have been performed at the BP86/A level, by numerical differentiation of analytical first derivatives.

Additional single-point Hartree−Fock, MP2, and coupled-cluster (CCSD and CCSD(T)) energy calculations at the BP86/A optimized structures employed an additional f-function ($\alpha = 0.823$)[24] on tungsten. The resulting basis will be denoted "B". These calculations have been carried out with the MOLPRO program system.[25] In the following, the computational levels will be denoted in the usual way,[26] e.g. CCSD(T)/B//BP86/A stands for a CCSD(T) single-point calculation with basis B at the structure optimized with the BP86 functional and basis A. Natural bond-orbital (NBO) analyses[27] used the built-in subroutines of Gaussian92/DFT.[22]

NMR ^{13}C and ^{1}H chemical shift calculations within the sum-over-states density-functional perturbation-theory approach (SOS-DFPT) in its Loc1 approximation[28] have been carried out for the BP86/A optimized structures **1** and **3**. These calculations used the same quasirelativistic tungsten ECP and valence basis[17] as the optimizations, but the IGLO-II all-electron basis sets[29] were used on carbon and hydrogen. We have recently shown this combination of quasirelativistic ECP on the metal with SOS-DFPT to be the first computational approach which gives accurate ligand NMR chemical shifts in heavy transition-metal complexes.[30−33] The NMR chemical shift calculations with a modified deMon[16] version used the exchange-correlation functional of Perdew and Wang,[34] a "FINE" grid,[16] and auxiliary bases of the size 3,4 (W), 5,2 (C), and 5,1 (H) (*n*,*m* denotes *n* s-functions and *m* spd-shells). The SOS-DFPT calculations employed individual gauges for localized orbitals (IGLO).[29] Chemical shifts are given with respect to $Si(CH_3)_4$ (TMS), optimized and calculated at the same computational level (the absolute shieldings of carbon and hydrogen in TMS at this level are 187.5 and 31.0 ppm, respectively).

III. Results and Discussion

A. Relative Energies of Different Structures. Table 1 compares relative energies calculated for the different structures (cf. Figure 1) at various computational levels. It also gives the number of imaginary frequencies obtained in the BP86/A harmonic frequency analyses. In agreement with the work of Kang et al.,[8] the "octahedral" D_{3d} structure **6** is very high in energy and may definitely be excluded as a stable structure. It exhibits ten imaginary frequencies. The distorted octahedral C_{3v} structure **5** is much more favorable, but still much higher in energy than structures derived from a trigonal prism, again in agreement with previous results.[8] It is a transition state with a low (90 cm^{-1}) imaginary frequency corresponding to methyl-group rotation. Interestingly, a BP86/A optimization starting at **5**, with symmetry constraints relaxed to C_3, did not lead to a nearby local distorted octahedral minimum as we expected, but back to the distorted trigonal prismatic C_3 minimum **1** (cf. below).

At all three correlated levels employed for the structure optimizations (BP86/A, B3P86/A, MP2/A) the trigonally distorted C_{3v} structure **2** (Figure 1b) is found, which Kang et al. could not observe in their Hartree−Fock structure optimizations. All electron-correlated methods, including the CCSD(T)/B//BP86/A computations, agree that structure **2** is ca. 12−22 kJ mol^{-1} more stable than the regular trigonal-prismatic D_{3h} structure **4** favored by Kang et al.[8] and by Haaland et al.[12] In contrast, the Hartree−Fock/B//BP86/A calculations would favor the D_{3h} structure **4** over the distorted structure **2** (Table 1). Thus, obviously electron correlation is important for the stability of **2**

(22) Gaussian 92/DFT, Revision G, Frisch, M. J.; Trucks, G. W.; Head-Gordon, M.; Gill, P. M. W.; Wong, M. W.; Foresman, J. B.; Johnson, B. G.; Schlegel, H. B.; Robb, M. A.; Replogle, E. S.; Gomperts, R.; Andres, J. L.; Raghavachari, K.; Binkley, J. S.; Gonzalez, C.; Martin, R. L.; Fox, D. I.; DeFrees, D. J.; Baker, J.; Stewart, J. P.; Pople, J. A. Gaussian, Inc.: Pittsburgh, PA, 1992.

(23) Becke, A. D. *J. Chem. Phys.* **1993**, *98*, 5648.

(24) Ehlers, A. W.; Böhme, M.; Dapprich, S.; Gobbi, A.; Höllwarth, A.; Jonas, V.; Köhler, K. F.; Stegmann, R.; Veldkamp, A.; Frenking, G. *Chem. Phys. Lett.* **1993**, *208*, 111.

(25) Program system MOLPRO (MOLPRO92 and MOLPRO94), written by Werner, H. J.; Knowles, P. J., with contributions by Almlöf, J.; Amos, R.; Elbert, S.; Hampel, C.; Meyer, W.; Peterson, K.; Pitzer, R.; Stone, A.

(26) Explanations of standard levels of ab initio MO theory, such as the Hartree−Fock (HF) and MPn methods, may be found, e.g., in: Hehre, W. J.; Radom, L.; Schleyer, P. v. R.; Pople, J. A. *Ab Initio Molecular Orbital Theory*; Wiley: New York, 1986.

(27) Reed, A. E.; Curtiss, L. A.; Weinhold, F. *Chem. Rev.* **1988**, *88*, 899.

(28) (a) Malkin, V. G.; Malkina, O. L.; Casida, M. E.; Salahub, D. R. *J. Am. Chem. Soc.* **1994**, *116*, 5898. (b) Malkin, V. G.; Malkina, O. L.; Eriksson, L. A.; Salahub, D. R. In *Theoretical and Computational Chemistry*; Politzer, P., Seminario, J. M., Eds.; Elsevier: Amsterdam, 1995; Vol. 2.

(29) Kutzelnigg, W.; Fleischer, U.; Schindler, M. In *NMR−Basic Principles and Progress*; Springer Verlag: Heidelberg, 1990; Vol. 23, p 165.

(30) Kaupp, M.; Malkin, V. G.; Malkina, O. L.; Salahub, D. R. *Chem. Phys. Lett.* **1995**, *235*, 382.

(31) Kaupp, M.; Malkin, V. G.; Malkina, O. L.; Salahub, D. R. *J. Am. Chem. Soc.* **1995**, *117*, 1851.

(32) Kaupp, M.; Malkin, V. G.; Malkina, O. L.; Salahub, D. R. *Chem. Eur. J.* **1996**, *2*, 24.

(33) (a) Kaupp, M. *Chem. Eur. J.* **1996**, *2*, 194. (b) Kaupp, M. *Chem. Ber.* In press.

(34) Perdew, J. P.; Wang, Y. *Phys. Rev.* **1992**, *B45*, 13244. Perdew, J. P.; Chevary, J. A.; Vosko, S. H.; Jackson, K. A.; Pederson, M. R.; Singh, D. J.; Fiolhais, C. *Phys. Rev. B* **1992**, *46*, 6671.

(of course also for **1**). This explains why Kang et al. could not find structure **2** in their Hartree−Fock optimizations.

However, even structure **2** exhibits three imaginary frequencies (around 100 cm^{-1}) corresponding to rotations of methyl groups. Therefore, we have carried out an optimization in C_3 symmetry (structure **1**) which indeed converged to a slightly lower energy than **2**, both at BP86/A (3.2 kJ mol^{-1}) and at MP2/A (0.6 kJ mol^{-1}). The methyl groups are only rotated very slightly (cf. below) with respect to **2** (Figure 1a). The D_{3h} structure **4** also may distort to a D_3 structure **3** by methyl-group rotation. However, the energy gain for **4** → **3** is even smaller than for **2** → **1**. Probably, there is almost free rotation of the methyl groups in $W(CH_3)_6$. Not too much significance should be attached to the imaginary frequencies in the vibrational analysis for **2**. The D_3 structure **3** is a transition state connecting two different C_3 minima **1**. The calculated barrier for this umbrella motion of **1** is only ca. 12−22 kJ mol^{-1}, i.e. close to the range of thermal energies at room temperature or above. This is of significance for the interpretation of the NMR spectra (cf. below), and for the structure determination by gas-phase electron diffraction. In both cases, the presence of low-energy large-amplitude vibrations has to be kept in mind (in agreement with the molecular-mechanics results of Landis et al.[13]).

B. Structures and Agostic Interactions. As BP86/A, B3P86/A, and MP2/A structure optimizations generally gave almost identical results (see e.g. table in the supporting information), only BP86/A results are shown in Figure 1. The computed bond distances of **3** and **4** also agree well (the W−C bonds of Figure 1c,d are a few pm longer) with the results of the HF optimizations by Kang et al.,[8] and with the GED data.[12] However, we find that the C−H bonds and H−C−W angles are far from uniform, particularly for the less symmetrical structures (e.g. **1**, **2**, **5**). They have been assumed to be equivalent in refs. 8 and 12.

The difference between the smaller (W−C1) and larger (W−C4) bond lengths of **1** (or **2**) is ca. 0.06 Å. The tetrahedron composed of W, C1, C2, and C3 features considerably larger C−W−C angles (ca. 95°) than the W−C4−C5−C6 part of the molecule (ca. 76°). Compared to the ideally C_{3v} symmetrical structure **2**, the methyl groups are rotated only very slightly: methyl groups 1−3 by 5.4 (7.1°) and methyl groups 4−6 by 3.3° (4.3°) at the BP86/A (MP2/A) levels, consistent with the very small energy difference between **1** and **2**.

The agostic C−H → W interactions mentioned in the introduction are apparent from the C−H distances and H−C−W angles, but also from the range of W−H distances (Figure 1a). The situation is different for the two different types of methyl groups present in **1**: For methyl groups 1−3 (cf. Figure 1a), the axial C1−H1 bond is considerably longer than the two equatorial bonds, and the axial angle is much smaller than the two equatorial ones (with corresponding reduced W−H1 and extended W−H2 and W−H3 distances). In contrast, for methyl groups 4−6, the two equatorial C−H bonds are elongated and the H−C−W angle is compressed. This indicates that the three upper methyl groups 1−3 exhibit agostic interactions due to the axial C−H groups but the lower methyl ligands 4−6 prefer (somewhat less pronounced) donation from the equatorial C−H bonds to the metal. The regular trigonal-prismatic structures **3** and **4** also feature nonidentical C−H distances and H−C−W angles for axial and equatorial hydrogens, but to a lesser extent (Figures 1c,d).

In attempting to obtain a rough energy estimate of the role that these hyperconjugative interactions play for the structural preferences of $W(CH_3)_6$, constrained optimizations for arrangements **2** and **4** have been carried out at the BP86/A level, restricting all methyl groups to an idealized structure with all C−H distances being 1.104 Å and all H−C−W angles being 111.5°. These partial optimizations led to total energies that were ca. 13 kJ mol^{-1} above the fully optimized structure for **2** but only ca. 2 kJ mol^{-1} higher for **4** (consistent with the smaller structural distortions of the methyl groups in **4** compared to **2**; see above and Figure 1). These results suggest that the structural changes due to agostic interactions favor the distortion **4** → **2** (or **3** → **1**) of $W(CH_3)_6$. The fact that the agostic interactions are dependent on electron correlation may be partly responsible for the absence of this distortion at the Hartree−Fock level of theory (cf. bonding discussion in section III.D).

Table 2. Comparison of Relative Energies (kJ mol^{-1}) for Different Structures of $W(CH_3)_6$ and WH_6[a]

structure	$W(CH_3)_6$	WH_6	comment
1	0.0 (C_3)	0.0 (C_{3v})	dist trig prism
3	+24.6 (D_3)	+153.3 (D_{3h})	reg trig prism
5	+131.9 (C_{3v})	+34.9 (C_{3v})	dist octahedron
6	+374.7 (D_{3d})	+661.9 (D_{3d})[b]	reg octahedron
7		+1.9 (C_{5v})	pentagonal pyramid

[a] BP86/A results (with an additional p-function on hydrogen for WH_6, see text). [b] Essentially octahedral structure (less than 1° deviation in angles).

Results of the BP86/A optimizations for the distorted octahedral structure **5** are indicated in Figure 1e. The two sets of methyl groups in this structure differ even more than in **1**, both in terms of distances and angles. The metal exhibits almost planar coordination by C4, C5, and C6. The structural distortions for these three methyl groups are also particularly large. Structure **6** is close to an ideal octahedron with C−W−C angles close to 90°.

C. Differences and Similarities to WH_6. The above results for different stationary points of $W(CH_3)_6$ indicate similarities to those found previously for WH_6,[8,9] as both species apparently favor distorted trigonal-prismatic C_{3v}-symmetrical WX_6 skeletons. However, there are significant differences, both in structures and in relative energies.

Table 2 compares the relative energies for different stationary points on the WX_6 (X = CH_3, H) potential-energy surfaces (the results for WH_6 are comparable to those of previous ab initio calculations[8,9]). Both molecules feature distorted trigonal-prismatic structures **1** (of C_{3v} symmetry for WH_6, of C_3 symmetry for $W(CH_3)_6$) as the most stable ones. However, the relative energy ordering of the regular trigonal-prismatic and distorted octahedral structures (**3** vs **5**) is reversed. Thus, the energy gain from a trigonal distortion of the regular prism is much less with the more bulky methyl ligands (25 vs 150 kJ mol^{-1}). The distortion of the regular octahedral structure **6** either to **5** or to trigonal-prismatic arrangements **1** or **3** also provides somewhat less energy gain for X = CH_3. The distorted octahedral structure **5** is considerably less competitive (compared to **1** or **3**) than that for the hydride.

The smaller energy gain for $W(CH_3)_6$ from a distortion of the regular trigonal prism **3** → **1** is also reflected in the structural details. Figure 2 shows the corresponding BP86/A optimized structure of WH_6, which is in good agreement with previous calculations.[8,9] The angular distortion is much more pronounced for the hydride than for the methyl complex (cf. Figures 1a and 2). Interestingly, the W−X bonds on that side of the complex with the compressed X−W−X angles (X = H4 through H6) are the shorter ones, while the situation is reversed for $W(CH_3)_6$.

One structure, which we have not considered in the present study on the hexamethyl complex, but which is competitive for WH_6,[8,9] is the pentagonal pyramidal isomer **7** (Table 2). Due to the very close approach of the ligands in the basal plane,

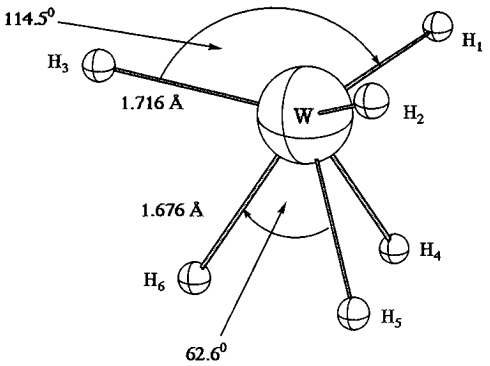

Figure 2. BP86/A optimized structure of the trigonal-prismatic C_{3v} minimum **1** of WH_6 (p-functions on hydrogen added, $\alpha = 1.0$).

Table 3. NBO Analysis for Different Structures of $W(CH_3)_6$[a]

	1 (C_3)	**3** (D_3)	**5** (C_{3v})	**6** (D_{3d})
Q(W)[b]	1.148	1.362	0.971	1.981
6s(W)[c]	0.477	0.490	0.468	0.567
6p(W)[c]	0.012	0.014	0.010	0.019
$5d_{xy}$, $5d_{x^2-y^2}$	0.787	0.810	0.847	0.656
$5d_{xz}$, $5d_{yz}$	1.131	1.133	0.960	0.891
$5d_{z^2}$	0.561	0.271	0.974	0.339
total 5d(W)[c]	4.370	4.126	4.570	3.433
$Q(CH_3)$[b]				
C1[d]	−0.215	−0.227	−0.135	−0.330
C4[d]	−0.168	−0.227	−0.189	−0.330
hyb (W−C)[e]				
W−C1[d]	$sd^{6.7}$	$sd^{7.6}$	$sd^{9.9}$	$sd^{4.3}$
W−C4[d]	$sd^{11.4}$	$sd^{7.6}$	$sd^{9.1}$	$sd^{4.3}$

[a] Based on Kohn−Sham orbitals at the BP86/A level. [b] Partial atomic charge. [c] Valence populations. [d] See Figures 1a,c,e,f for atomic labels. [e] Hybridization analysis of metal NAO contributions to the W−C bonding NLMOs. p-Orbital contributions are negligible.

Table 4. NBO Analysis for Different Structures of WH_6[a]

	1 (C_{3v})	**3** (D_{3h})	**5** (C_{3v})	**6** (D_{3d})	**7** (C_{5v})
Q(W)[b]	0.230	0.940	−0.016	2.292	0.255
6s(W)[c]	0.743	0.828	0.679	0.954	0.746
6p(W)[c]	0.013	0.051	0.017	0.145	0.013
$5d_{xy}$, $5d_{x^2-y^2}$	0.751	0.803	1.030	0.435	1.360
$5d_{zz}$, $5d_{yz}$	1.376	1.231	1.096	0.870	0.761
$5d_{z^2}$	0.803	0.006	1.119	0.000	0.788
total 5d(W)[c]	5.075	4.074	5.371	2.610	5.030
Q(H)[b]					
H1[d]	−0.105	−0.157	+0.087	−0.382	−0.148
H4[d]	+0.028	−0.157	−0.081	−0.382	−0.021
hyb (W−H)[e]					
W−H1[d]	$sd^{4.3}$	$sd^{5.1}$	$sd^{14.5}$	$sd^{2.8}$	$sd^{3.1}$
W−H4[d]	$sd^{12.5}$	$sd^{5.1}$	$sd^{5.0}$	$sd^{2.8}$	$sd^{8.1}$

[a] Based on Kohn−Sham orbitals at the BP86/A level. [b] Partial atomic charge. [c] Valence populations. [d] The atomic labeling is analogous to that for $W(CH_3)_6$ (see Figures 1a,c,e,f). For structure **7** (C_{5v}), H1 denotes the apical and H4 the basal ligand. [e] Hybridization analysis of metal NAO contributions to the W−H bonding NLMOs. p-Orbital contributions are negligible.

this arrangement is likely to be very unfavorable for the methyl compound.

D. Bonding Analysis. Insight into the origin of the differences between $W(CH_3)_6$ and WH_6 is provided by comparative natural population and natural bond orbital analyses (NPA, NBO[27]). Tables 3 and 4 summarize the partial charges, metal valence populations, and results of a hybridization analysis of the W−X bonding natural localized molecular orbitals (NLMO) for different structures of the methyl and hydride complexes, respectively.

Consistent with the smaller structural and energetic differences between different arrangements for the methyl complex, the bond ionicities (cf. NPA charges Q(M) and Q(X)) vary over a smaller range than for the hydride. In both cases, the most ionic situation is represented by the regular octahedral structure whereas the more stable arrangements have, e.g., smaller metal charges and larger d-orbital contributions to the W−X bonds. This result agrees with previous arguments which relate the preference for the less symmetrical structures to an improved involvement of the metal d-orbitals in covalent σ-bonding.[8,9] However, maximization of covalent bonding and d-orbital participation alone would in both cases favor the distorted octahedral structure **5** (Tables 3 and 4). This ligand arrangement must be disfavored by strong repulsive interactions, particularly for the methyl complex.

Interestingly, agostic interactions appear to increase the preference for a trigonal distortion in $W(CH_3)_6$ (cf. section III.B), whereas π-donation contributions from nonbonding ligand orbitals, e.g. in WF_6[8,9] (which should be analogous with respect to orbital symmetry considerations), favor more symmetrical structures. These differences may be related to the fact that the agostic interactions involve changes in the W−C−H angles and C−H distances and also depend on the orientation of the methyl groups. Apparently, by these small structural changes the methyl groups adapt so well to the skeletal distortions in **1** or **2** that the overall effect is in favor of the distortion.

Upon going from the octahedron **6** to the trigonal prism **3**, the populations of the d_{xy}, $d_{x^2-y^2}$ and of the d_{xz}, d_{yz} sets both increase (in the simple one-electron picture given in ref 8, only the former set was considered), whereas the s- and p-populations decrease. The further distortion of the regular trigonal prism **3** to **1** is mainly accompanied by an increase in the d_{z^2} populations, again in agreement with arguments given previously.[8] The major difference between the methyl and the hydride complexes is that the former already exhibits an appreciable population of this orbital in **3** but the latter does not (this holds also for **6**, cf. Table 4). This population is partly connected to the agostic delocalization contributions (i.e. to σ-C−H → d_{z^2}(W) donation). However, the more directional character of the hybrid orbital provided for C−M bonding by the methyl ligand also appears to allow better overlap with the metal d_{z^2} acceptor orbital compared to a hydrogen 1s AO (the relative d_{z^2} populations are reversed for the distorted structure **1**, cf. Tables 3 and 4). This difference influences the structural preferences, as a smaller structural distortion suffices to electronically "saturate" the metal center in the methyl complex. Figure 3 shows the energy diagrams of the frontier Kohn−Sham MOs in $W(CH_3)_6$ (Figure 3a) and in WH_6 (Figure 3b) for regular vs distorted trigonal-prismatic structures. Obviously, in the regular trigonal prismatic structure the energy gap between the a_2 (a_2') HOMO (with significant ligand character) and the a_1 (a_1') LUMO (with predominantly metal d_z^2 character[8]) is larger with methyl (Figure 3a) compared to hydride (Figure 3b) ligands. Thus, the driving force for distortion via mixing of these two levels is reduced for the methyl complex. This explains at least in part the larger distortion for WH_6. Due to the considerably larger resulting distortion in the hydride, the changes in the orbital levels upon symmetry lowering are also more dramatic (e.g., the empty a_1 level in the C_{3v} structure ends up above the e-level, see Figure 3b).

The energies of all occupied Kohn−Sham orbitals (also of those not shown in Figure 3) except for the HOMO increase upon going from the regular to the distorted trigonal-prismatic structure. This holds for both species and contrasts with the simple one-electron picture given by Kang et al.[8] where only one valence orbital is destabilized and one stabilized, but the others remain unperturbed. Doubtlessly, strong repulsive

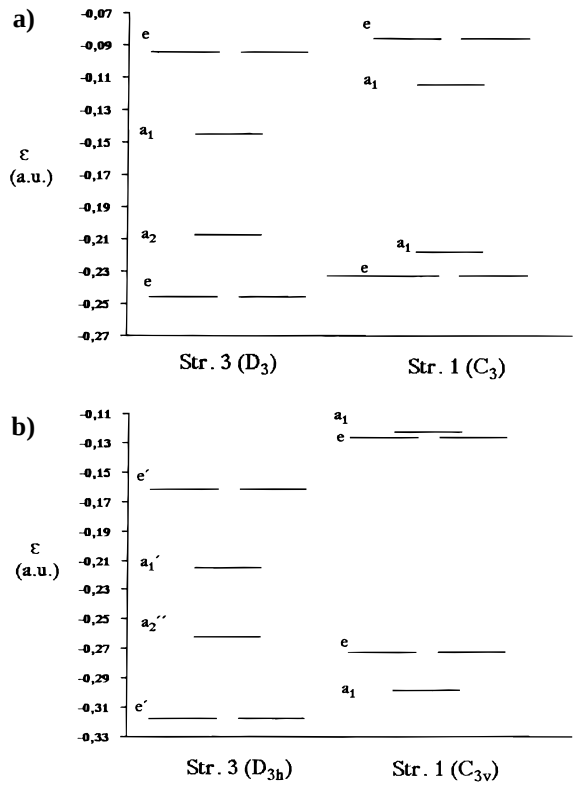

Figure 3. KS orbital-energy diagram for frontier MOs in regular and distorted trigonal-prismatic structures: (a) $W(CH_3)_6$ and (b) WH_6.

interactions oppose the compression of one side of the prism. For a given angular arrangement, these are likely to be more pronounced in the methyl complex.

The discussion of the relative weight of covalent and ionic bonding contributions in $W(CH_3)_6$ is not straightforward. Thus, e.g., the two nonequivalent sets of W−C bonds in **1** have quite different bonding environments: the shorter W−C1 bond on the less compressed side of the distorted prism is *less* covalent (cf. *Q*(C)) and exhibits *smaller* metal d-orbital contributions than the W−C4 bond. A similar situation holds for the distorted-octahedral structure **5**: The shorter W−C4 bond (again on the less compressed side of the coordination polyhedron) is the less covalent one. In contrast, for arrangement **1** of WH_6, the shorter $W-H_4$ bond (Figure 2) also is the more covalent one (Table 4). There seems to be a delicate balance between maximization of covalent bonding contributions and minimization of repulsive interactions in both species.

Agostic C−H → W interactions, as discussed in section III.B, are accompanied by slightly reduced C−H bond orders, and by somewhat larger tails of the corresponding C−H bonding NLMOs at the metal. A perturbation theoretical analysis[27] of interactions between C−H bonding NBOs and W−C antibonding or metal-centered "Rydberg-type"[27] NBOs also reveals slightly larger interactions for those C−H bonds exhibiting the smaller H−C−W angles and larger C−H distances (cf. section III.B). However, the overall contributions remain small.

E. NMR Chemical Shifts. Experimentally, only a single peak (with satellites due to spin−spin coupling) is found in the ^1H and in the ^{13}C NMR spectra (at 1.78 and 83.1 ppm, respectively) of $W(CH_3)_6$ at room temperature.[12,14] This is consistent either with a structure having six symmetrically equivalent methyl groups (e.g. like **3**) or with a fluctuating structure based on **1**. In view of the small computed barrier for the inversion **1** → **3** → **1** (Table 1), obviously the latter possibility must hold true.

Table 5. Calculated ^{13}C Chemical Shift Tensors (ppm vs TMS) for $W(CH_3)_6$

atom	δ_{11}	δ_{22}	δ_{33}	δ_{av}	$(\delta_{11}+\delta_{22})/2 - \delta_{33}$[c]
1[a]					
C1	79.6	68.6	11.7	53.3	62.4
C4	95.8	88.5	29.6	71.3	62.6
3[b]					
C1	94.3	79.8	30.2	68.1	56.9

[a] Figure 1a. [b] See Figure 1c. [c] Shift anisotropy.

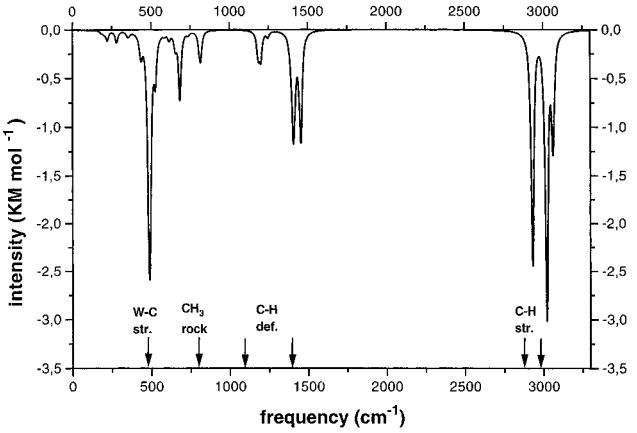

Figure 4. Simulated IR spectrum of $W(CH_3)_6$ (C_3 structure **1**) at the BP86/A level. The calculated harmonic vibrational frequencies and intensities have been convoluted by Lorenzians of line width 10 cm^{-1}. Arrows indicate the positions of the experimental maxima, with their assignments.[14]

The ^{13}C spectrum of $W(CH_3)_6$ originally initiated our interest in this species, as it exhibits one of the largest methyl ^{13}C shifts known. The calculated carbon shift tensors for **1** and **2** are shown in Table 5. The two nonequivalent sets of carbon atoms in **1** have isotropic shifts differing by ca. 18 ppm. Their computed average of ca. 62 ppm is lower than the experimental value, and so is the value of ca. 68 ppm obtained for structure **3**. This is consistent with our previous experience for d^0 species with a small gap between occupied and virtual orbitals[31] ($W(CH_3)_6$ is red[14]). Thus, the accuracy of the calculated shifts alone does not allow us to distinguish between a static structure **3** or a fluctuating structure **1**, the latter of which is favored on energetic grounds (Table 1). However, experiments at low temperatures might resolve the two nonequivalent sets of methyl groups for structure **1**. The computed shift difference of 18 ppm is more reliable than the shifts themselves. As it depends strongly on the magnitude of the structural distortion, this value provides an interesting possibility for an independent experimental confirmation of the computed structure.

The ^{13}C shift tensors have approximately axial symmetry, with $\delta_{\parallel} > \delta_{\perp}$. Decomposition of the tensors into contributions from individual localized MOs (LMOs) indicates significant paramagnetic contributions from a C−W σ-bonding LMO, but also from the C−H bonds. Most probably, the small energy gap between occupied and virtual electronic levels in $W(CH_3)_6$ largely accounts for these large paramagnetic contributions, and thus for the large ^{13}C shifts. The calculated proton shifts range from ca. 1.5 ppm to ca. 2.5 ppm. Those hydrogen atoms which are involved in agostic interactions exhibit shifts at the higher end of this range, the others at the lower end. Of course, rotation of the methyl groups averages these signals, and it is unlikely that one could sufficiently freeze this rotation.

F. Harmonic Vibrational Frequency Analysis. Figure 4 shows the simulated IR spectrum for $W(CH_3)_6$ obtained by convoluting the harmonic vibrational frequencies and intensities

(at the BP86/A level) with Lorenzian functions of halfwidth 10 cm^{-1}. The peaks identified by Shortland and Wilkinson[14b] (see arrows in Figure 4) are reasonably well reproduced by the calculations, with a slight overestimate by ca. 5%. Thus, a scaling factor of ca. 0.96 would bring theoretical and experimental data into excellent agreement. Unfortunately, the IR spectrum has only limited value for the structure assignment, as the alternative structural possibilities lead to peaks in the same regions. This restriction also holds for the photoelectron spectra[35] and is probably in part responsible for the fact that $W(CH_3)_6$ was thought to be octahedral for ca. 20 years after its first characterization.[14a]

IV. Conclusions

Like its hydride analogue WH_6, hexamethyltungsten, $W(CH_3)_6$, adopts a distorted trigonal-prismatic structure with a C_{3v} WX_6 backbone. Due to a slight twisting of the methyl ligands, the overall symmetry of the minimum structure is C_3. Electron correlation and C−H → W agostic interactions are important for the distortion from the regular prism, by alleviating repulsions between the methyl groups. This is the reason why a previous computational study, based on Hartree−Fock optimizations, came to the conclusion that the structure is regular trigonal prismatic. Gas-phase electron diffraction could not differentiate between these two possibilities, as the $C_3 \rightarrow D_3 \rightarrow C_3$ transformation requires only ca. 12−22 kJ mol^{-1} (this is much less than the ca. 109 kJ mol^{-1} computed for WH_6). Thus, at elevated temperatures, the molecule doubtlessly carries out large-amplitude "umbrella-type" vibrations. Interestingly, the molecular-mechanics/valence-bond scheme of Landis et al.[13] agrees with our ab initio and DFT results by giving a moderately distorted trigonal prism for $W(CH_3)_6$, and even their inversion barrier is within the range indicated above. Preliminary molecular dynamics simulations apparently give[13] internuclear radial distributions consistent with the GED data of ref 12.

The driving force for the distortion $O_h \rightarrow D_{3h} \rightarrow C_{3v}$ of d^0 ML_6 complexes has been rationalized previously on the basis of improved overlap between ligand orbitals and metal d-orbitals,[8,9] similar to discussions for other cases of symmetry reduction for d^0 species.[1−12] However, more subtle details can also influence the structural preferences, as indicated, e.g., by our population analyses for structure **5** (section III.D). Apart from increased d-orbital σ-bonding contributions for the less symmetrical structures, as well as π-bonding and repulsive interactions between the ligands, which are more effective for higher symmetry,[1−5,8−10] a polarization of the $(n-1)$p semicore orbitals has to be considered.[1−3] The efficient involvement of the d-orbitals in bonding is impossible without a simultaneous relaxation of the underlying p-orbitals, due to their similar radial extent. Therefore, d-orbital involvement and core polarization are interrelated and not strictly separable.[36] For $W(CH_3)_6$, secondary hyperconjugative ("agostic") σ-C−H → W interactions also influence the competitiveness of different nuclear arrangements. We find significant differences between these interactions and comparable "regular" π-bonding contributions, e.g. in WF_6.

Calculated NMR chemical shifts agree moderately well with experiment if a fluctuating structure is assumed and the shift values computed for structure **1** are averaged. The computed ^{13}C shift difference of 18 ppm between the nonequivalent carbon atoms in **1** may suggest a low-temperature NMR study as an experimental tool to validate the distorted C_3 arrangement.

Preliminary computations indicate that the experimentally unknown $Mo(CH_3)_6$ has the same C_3 structure **1** as its tungsten analogue.[37] In contrast, at the same computational levels, the d^1 complex $Re(CH_3)_6$ appears to have the regular trigonal-prismatic D_3 structure **3**.[37]

Acknowledgment. I am grateful to Deutsche Forschungsgemeinschaft (DFG) for a "Habilitationsstipendium" and to Prof. H. G. von Schnering (Max-Planck-Institut, Stuttgart) and Prof. H.-J. Werner (Universität Stuttgart) for their interest and for providing computational resources. The NMR chemical shift calculations have benefitted from recent progress made in cooperation with Dr. V. G. Malkin and O. L. Malkina (Bratislava), and with Prof. D. R. Salahub (Montréal) (refs 30−32). P. N. Roy (Montréal) kindly provided a program for the Lorenzian convolution of the IR data.

Note Added in Proof: After this paper had been accepted, a remarkable low-temperature single-crystal X-ray diffraction study of $W(CH_3)_6$ and $Re(CH_3)_6$ appeared (Pfennig, V.; Seppelt, K. *Science* **1996**, *271*, 626). The results of Pfennig and Seppelt for hexamethyltungsten confirm our computational structure prediction quantitatively (X-ray diffraction could not locate the hydrogen positions accurately and thus gives little information on the structural distortions due to agostic interactions or on the slight twisting of the methyl groups observed computationally). $Re(CH_3)_6$ has also been found to be distorted trigonal prismatic by Pfennig and Seppelt, but with smaller deviations from a regular prism. A very shallow potential-energy surface may be expected for the "umbrella-type" $C_3 \rightarrow D_3 \rightarrow C_3$ mode, and the correct computational description of the structural details will be more demanding than for closed-shell $W(CH_3)_6$.

Supporting Information Available: One table comparing computed structures at different levels of theory (1 page). This material is contained in many libraries on microfiche, immediately follows this article in the microfilm version of the journal, can be ordered from the ACS, and can be downloaded from the Internet; see any current masthead page for ordering information and Internet access instructions.

JA952231P

(35) Green, J. C.; Lloyd, D. R.; Galyer, L.; Mertis, K.; Wilkinson, G. *J. Chem. Soc., Dalton Trans.* **1978**, 1403.

(36) Kaupp, M. Dissertation, Universität Erlangen−Nürnberg, 1992.

(37) Kaupp, M. Unpublished results.